Thermal hysteresis phenomena and mesoscopic phase coexistence around the neutral-ionic phase transition in TTF-CA and TMB-TCNQ

M. Buron-Le Cointe, M. H. Lemée-Cailleau, H. Cailleau, B. Toudic, and A. Moréac
Groupe Matière Condensée et Matériaux, UMR au CNRS 6626, Université Rennes 1, Bât. 11A Campus de Beaulieu, 35042 RENNES Cedex, France

F. Moussa
Laboratoire Léon Brillouin, Laboratoire Commun CEA-CNRS, CEN Saclay, 91191 Gif Sur Yvette Cedex, France

C. Ayache
CEA/Direction des Sciences de la Matière, L'Orme des Merisiers, CEA Saclay, 91191 Gif Sur Yvette Cedex, France

N. Karl
3. Physikalisches Institut, Universität Stuttgart, D-70550 Stuttgart, Germany
(Received 10 July 2002; revised manuscript received 25 March 2003; published 7 August 2003)

Hysteresis phenomena are investigated around the temperature-induced neutral-ionic (*N-I*) phase transition in the prototype compound tetrathiafulvalene-*p* chloranil (TFF-CA). A multistep transition is evidenced by neutron scattering, with plateau evolution of Bragg peaks characteristic of symmetry breaking, as well as by specific heat measurements revealing a multipeak structure, both in perfect agreement. A structural study reveals the coexistence of *N* and *I* phases at a mesoscopic scale during the thermal hysteresis. No gradual process with intermediate long periodicity structure based on alternating *N* and *I* planes, as theoretically suggested, takes place. These results, supported by optical microscopy studies performed on both TTF-CA and tetramethylbenzidine-tetracyanoquinodimethane (TMB-TCNQ) crystals, underline the importance of interstack elastic coupling at the temperature-induced neutral-ionic transition.

DOI: 10.1103/PhysRevB.68.064103 PACS number(s): 61.50.Ks, 68.65.−k, 65.40.Gr, 07.60.Pb

INTRODUCTION

The great richness of organic molecular solids lies in the possibility to tune properties under external stimuli such as temperature, pressure or light, by playing on the coupling between electronic and structural parameters. Of particular interest are presently photoinduced transformations[1–9] where the relaxation of optically excited states results in large transformed domains, up to a macroscopic scale, with the new electronic order being accompanied by a new structural one (change of both intramolecular geometries and intermolecular organization, i.e., lattice relaxation). Strongly coupled electronic-structural changes can also affect the electrical transport properties and even lead to switching between low and high conductivity states when a sufficiently large electric field is applied (so-called negative resistance effect[10–13]). Both photoinduced and high-electric-field-induced transformations allow prospects in the future development of molecular devices in electronics or optoelectronics, and it is a real challenge to understand and control the cooperativity between lattice-relaxed excited states in order to be able to optimize the desired switching between different molecular states.

Some mixed-stack CT complexes, that are composed of electron donor (*D*) and electron acceptor (*A*) molecules, undergo an equilibrium neutral-ionic (*N-I*) phase transition under application of pressure or, more rarely, upon lowering temperature.[14–19] Out of equilibrium photoinduced and high-electric-field-induced transformations are reported for the prototype compound tetrathiafulvalene-*p* chloranil (TTF-CA).[5–11] Fully *N* and fully *I* chains are commonly represented as $\cdots D^{\circ}A^{\circ}D^{\circ}A^{\circ}D^{\circ}A^{\circ}D^{\circ}A^{\circ}\cdots$ and $\cdots D^{+}A^{-}D^{+}A^{-}D^{+}A^{-}D^{+}A^{-}\cdots$, respectively. Lattice relaxation manifests itself by molecular distortions and the formation of *DA* pairs in the *I* phase,[20] i.e., by an alternation of two different distances along the chain, whereas *D* and *A* regularly alternate in the *N* phase. The conventional schematic representations are

$$\cdots(D^{+}A^{-})(D^{+}A^{-})(D^{+}A^{-})(D^{+}A^{-})\cdots$$

$$\text{or } \cdots(A^{-}D^{+})(A^{-}D^{+})(A^{-}D^{+})(A^{-}D^{+}\cdots$$

for fully *I* dimerized chains. The phase transition is governed by the formation of lattice-relaxed (LR) charge-transfer (CT) exciton strings, first theoretically introduced by Nagaosa.[21] These non-linear excitations are either several adjacent dimerized ionic molecular $(D^{+}A^{-})$ pairs inserted in a *N* chain (the system is globally in the centrosymmetric *N* phase), or several adjacent undimerized neutral molecular $D^{\circ}A^{\circ}$ pairs inserted in an *I* dimerized chain (the system is globally in the *I* ferroelectric phase). These non-linear excitations are conventionally represented by

$$\cdots D^{\circ}A^{\circ}D^{\circ}A^{\circ}(D^{+}A^{-})(D^{+}A^{-})(D^{+}A^{-})D^{\circ}A^{\circ}\cdots.$$

The *N-I* phase transition has been analyzed as a cascade of cooperative multiscale phenomena:[22,23] First the formation of nano-CT strings accompanied by their one-dimensional (1D) lattice relaxation,[21] as recently evidenced by x-ray diffuse scattering,[24] and then their three-dimensional condensation

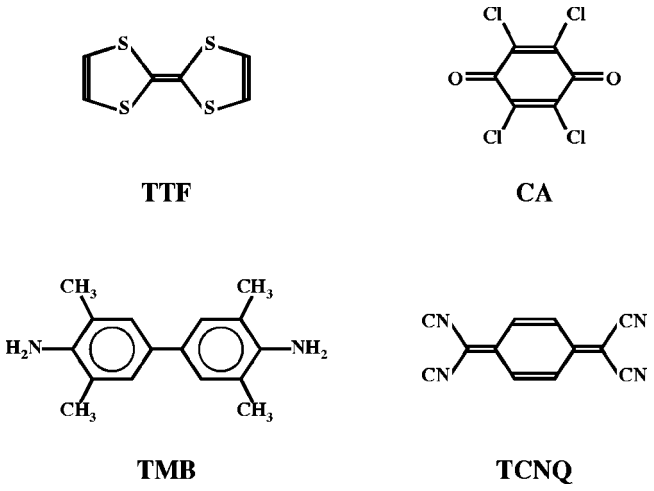

FIG. 1. Schematic drawing of the molecular structures of tetrathiafulvalene (TTF), p-chloranil (CA), tetramethylbenzidine (TMB), and tetracyanoquinodimethane (TCNQ).

and ordering (on a microscale),[25] leading to ferroelectricity phenomena driven by both charge and dimerization fluctuations.[26] Mixed-stack CT systems undergoing the *N-I* phase transition can then be viewed as model systems for extensive studies of LR-CT excitations and their cooperativity. Indeed, the equilibrium *N-I* phase transition is nothing else than a particular case of transformation where the cooperativity between the LR-CT excitations is carried to the extreme.

The aim of the present paper is to bring insight into the switching of molecular species by a precise examination of the coexistence of the *N* and *I* phases, and of hysteresis phenomena around the equilibrium temperature-induced *N-I* phase transition in two mixed-stack CT complexes, tetrathiafulvalene-*p* chloranil (TTF-CA), and tetramethylbenzidine-tetracyanoquinodimethane (TMB-TCNQ). (For the component molecules see Fig. 1.) These 1:1 stoichiometric compounds have in common a monoclinic symmetry (space group $P2_1/n$ with two *DA* pairs in the unit cell) for the high temperature *N* phase.[27,15] Each molecule is located on an inversion center and the mixed CT chains are parallel to the **a** unit-cell axis. At atmospheric pressure, the temperature-induced clear first-order transition[14,15,20,28–36] is characterized by the simultaneity of a bond dimerization process and a change of the molecular identities by partial CT. The two compounds differ by the transition temperature $T_{N\text{-}I}$, the ionicity jump $\Delta\rho$, and the hysteresis loop: TTF-CA,[28–33] $T_{N\text{-}I}=81$ K, $\Delta\rho=0.4\,e^-$, hysteresis loop across about 2–3 K, TMB-TCNQ,[15] $T_{N\text{-}I}=205$ K, $\Delta\rho=0.1\,e^-$, hysteresis loop across about 30 K. Taking into account both repulsive and attractive interstack Coulombic interactions (but not dimerization) and their possible frustrations, it has been theoretically suggested that ionization of the molecules would gradually occur via long period structures based on parallel fully *N* or *I* planes, in a multistep sequence of first-order transitions associated with a so-called Devil's staircase behavior.[37,38] Some experimental observations are in favor of this model, also called staging state: a plateau effect observed on the electric conductivity[31] as well as a multistep behavior of the specific heat anomaly[39] were reported for TTF-CA. For TMB-TCNQ a two-step pressure-induced *N-I* transition was observed from reflectivity spectra.[40] However, such techniques cannot provide information on a possible complex intermediate packing scheme during the multistep sequence. In what follows we present, on the one hand, structural investigations by neutron scattering, allowing a direct observation of the structural reorganization occurring during the hysteresis loop in TTF-CA; these investigations are supported by specific heat measurements performed on a set of two single crystals. On the other hand, these results are complemented by an optical microscopy study of the temperature-induced *N-I* transition of both TTF-CA and TMB-TCNQ.

EXPERIMENTAL

As for any first order transition, it is of primary importance to use high quality single crystals in the investigation of the coexistence phenomena around the *N-I* transition in order to reduce artificial hysteresis effects caused by impurities and defects as much as possible. Single crystals of TTF-CA and TMB-TCNQ, both dark and shiny, were prepared by a close to isothermal cosublimation method from presublimed commercial TTF and CA, or TMB and TCNQ powders, as previously described.[20]

Neutron scattering investigations were carried out for TTF-CA on triple-axis spectrometers installed on the cold source of the reactor Orphée at the Laboratoire Léon Brillouin (LLB). Experiments were performed on a $5\times3\times2\,\mathrm{mm}^3$ TTF-CA single crystal, in the $(\mathbf{a}^\star,\mathbf{b}^\star)$ scattering plane on 4F-1 spectrometer and in the $(\mathbf{b}^\star,\mathbf{c}^\star)$ scattering plane on G4-3 spectrometer. Wave vectors, collimation angles, and the filters used are given in the figure captions. The cryogenic equipment used on these spectrometers allowed a temperature accuracy better than 0.02 K.

For specific heat measurements a differential adiabatic and dynamical method was used, as described for former experiments on powder samples.[39] Here, sensitivity has been significantly improved and the relative precision reached about $2-5\times10^{-3}$ K over the 20–300 K temperature range. All contributions of heat absorption from the sample environment were registered in a reference work file and therefore a reference-cell was not necessary. Because an instability of the TTF-CA under reduced pressure was noticed as previously in Ref. 39, the two single crystals used, weighing together $m=74.25$ mg, were placed together into a copper capsule, that was closed with araldite glue under a helium gas flow. In this way, the pumping, necessary before reaching very low temperatures, was not directly acting on the material itself, and moreover, the surrounding helium gas contributed to improve thermalization of the sample. A vacuum of about 10^{-4} Pa was then established in the calorimeter and kept constant. The supplied power was regularly adjusted at different temperatures outside the transition region in such a way as to keep the heating rate constant. Several data collections were made for different controlled heating rates, as well as for the natural cooling processes in between.

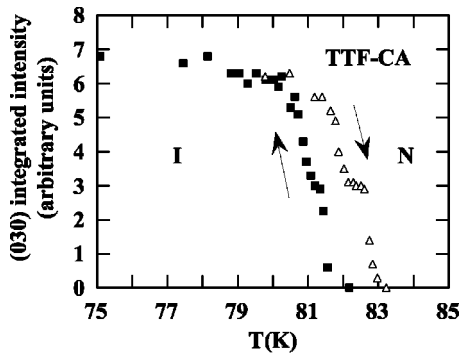

FIG. 2. Evolution with increasing (△) and with decreasing (■) temperature of the integrated intensity of the (030) reflection (arbitrary units). Symbols include error bars. Spectrometer 4F-1 at LLB; $k_i = k_f = 1.54\ \text{Å}^{-1}$ with a Be filter cooled to 77 K, collimations 40′/40′.

Optical microscopic investigations were performed under a polarization microscope (Laborlux Pol 12 Leitz) using tiny single crystals of TTF-CA and TMB-TCNQ, mounted in an Oxford microscope-cryostat that allowed studies down to helium temperature with a temperature stability better than 0.5 K. TTF-CA and TMB-TCNQ crystals were transparent (**a**, **b**) and (**a**, **c**) tablets, respectively, with dimensions of about $500 \times 100\ \mu\text{m}^2$ and a thickness of a few μm. Both materials present significant dichroism: TTF-CA and TMB-TCNQ are green and gray, respectively, when the light is polarized along the stacking axes **a**, yellow when it is polarized along **b** for TTF-CA and dark pink when it is polarized along **c** for TMB-TCNQ.

RESULTS

Structural aspects of the first-order temperature-induced *N-I* phase transition have been reported previously for the prototype compound TTF-CA,[20] focussing in particular on the nature of the symmetry-breaking and detailed structural changes in the *I* phase. The symmetry lowering is visible solely by the appearance of $k = 2n+1$ $(0k0)$ Bragg reflections at $T_{N\text{-}I}$, so that the definition of the Bravais lattice remains unchanged (space group $P2_1/n$, $Z=2$ for the *N* phase; *Pn*, $Z=2$ for the *I* phase). Figure 2 presents the evolution of the (030) reflection intensity measured on an unstressed crystal, with the $(\mathbf{a}^\star, \mathbf{b}^\star)$ reciprocal plane as scattering plane. In the present work the excellent temperature stability, allowing a well-resolved crossing of the transition, gave the opportunity to evidence both a hysteresis loop and a two-step behavior which was particularly well marked when temperature increased. Since the *N-I* transition at atmospheric pressure is strongly first order, the intensity of the $k = 2n+1$ $(0k0)$ characteristic reflections depends linearly on the concentration of the *I* phase in the *N-I* coexistence regime. The step is located approximately at half maximum of the saturated intensity value of the low-temperature *I* phase, marking the temperature range where half of the species are *N* and half are *I* ones. Theoretical models[37,38] predict a multistep transition with intermediate phases consisting of *I* layers inserted between *N* ones in order to reduce the intermolecular Coulombic repulsion. As Coulomb interactions are favorable along the chains from an electrostatic point of view, such long-range order packing would directly show up in the diffraction pattern by additional superstructure Bragg peaks along interstack directions. This situation was recently reported for a derivative of TTF-CA, 2,6 dimethyl TTF-CA (triclinic space group in both the high- and the low-symmetry phase, with **a** being the stacking axis too), where the periodic ordering between *N* and *I* (**a**, **b**) planes gives rise to a cell doubling along the **c** axis.[41] From the $P2_1/n$ symmetry of TTF-CA, in an approximation where the molecules are represented by points only, the most likely structure for a 50% *N*–50% *I* phase is a superstructure composed of alternating *N* and *I* layers parallel to the (011) plane [or to the $(01\bar{1})$ plane if domain formation is taken into account], as proposed for TMB-TCNQ from the observation of a plateau effect in the optical reflection spectra upon the pressure-induced transition.[40] Such an intermediate superstructure (Fig. 4 in Ref. 40) would lead to the doubling of both the **b** and the **c** cell parameters. In this hypothesis, the plateau observed with the (030) reflection (high-temperature lattice notation) would come from the doubling of the **b** cell parameter. Investigations in the $(\mathbf{b}^\star, \mathbf{c}^\star)$ scattering plane are necessary to confirm or disprove the existence of such an intermediate long-range ordered phase. Moreover, any other long-range ordered structure between *N* and *I* layers that might be imagined would lead to the appearance of superstructure reflections along at least one crystallographic axis [as observed in DMTTF-CA (Ref. 41)] and/or along the diagonals of the reciprocal plane $(\mathbf{b}^\star, \mathbf{c}^\star)$. Careful investigations along both $\mathbf{b}^\star$ and $\mathbf{c}^\star$ axis and along the diagonals of this plane, both before the transition and at the step level, unambiguously show that no superstructure reflection appears, and therefore disprove the existence of any intermediate long-range-ordered structure between *N* and *I* layers in TTF-CA. This is in perfect agreement with a recent *ab initio* calculation of the electrostatic energies in TTF-CA, using a point atom approximation, which leads to the conclusion that, the staging state is slightly less stable than uniform *N* or *I* states.[42]

The step phenomenon could also be a characteristic of an intergrowth of the *I* phase (low-symmetry *Pn*) into the *N* phase, without any multiplication of the unit-cell volume. The precise analysis of the diffraction patterns, observed in the $(\mathbf{a}^\star, \mathbf{b}^\star)$ and in the $(\mathbf{b}^\star, \mathbf{c}^\star)$ scattering planes, show a slight increase of ordinary $(0k0)$: $k = 2n$ Bragg peak widths during the sharp **b** jump, achieving their maximum at the plateau level. This increase has been resolved using the best spatial resolution of the G4-3 spectrometer at a neutron wave vector $k_i = 1.1\ \text{Å}^{-1}$ and 30′/30′ collimations. Figure 3(a) shows scans along $\mathbf{b}^\star$ across the (020) reciprocal lattice point. Two well-defined peaks are easily identifiable with, for both, a full width at half maximum expressing long-range order over the resolution limit of the spectrometer, i.e., over at least 1000 Å, that is more than 130 unit cells. They reflect the coexistence of *N* and *I* phases on a mesoscopic scale, each peak allowing the determination of a corresponding **b** cell parameter [Fig. 3(b)]. Such a coexistence extends across a temperature interval of about 2 K. Inside this interval the

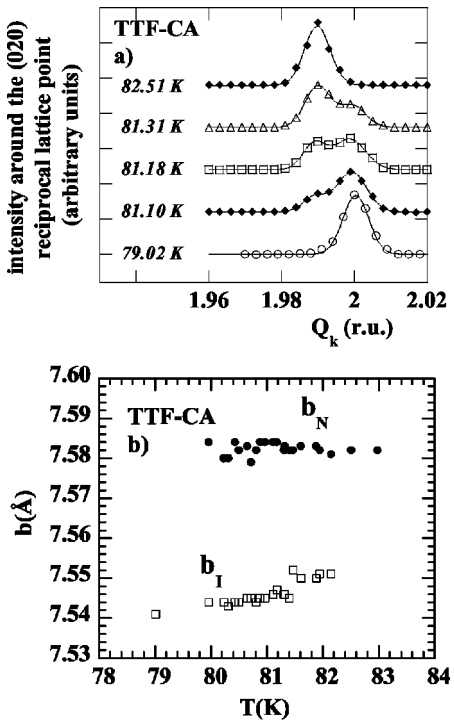

FIG. 3. (a) Evidence of a splitting of the (020) Bragg reflection in two. (b) **b** cell parameters of the neutral phase ($\mathbf{b}_N$), and of the ionic phase ($\mathbf{b}_I$), deduced from the double Bragg peak structure. All these measurements were made at increasing temperature; Spectrometer G4-3 at LLB; $k_i = k_f = 1.1$ Å^{-1} with a Be filter cooled to 77 K, collimations 30′/30′.

step phenomenon covers about 0.5–0.7 K; it is again well reproduced by following the respective fractions of each phase with the integrated intensities of related Bragg peaks (Fig. 4). The temperature ranges for the step phenomena as well as for the coexistence of the two phases at the mesoscopic scale are very reproducible. Nevertheless in the plateau the proportions of the *N* and *I* phases may vary, as concluded from the relative intensity of the (030) reflection (Fig. 2) or of the (020) reflection (Fig. 4). This behavior may have its origin in possible residual mechanical stress on the sample,

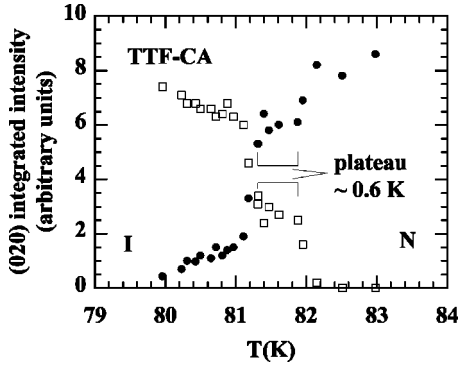

FIG. 4. Integrated intensities (arbitrary units) of the two (020) Bragg reflections detected at the transition. The measurements were made at increasing temperature; □ ionic phase, ● neutral phase. Spectrometer G4-3 at LLB; $k_i = k_f = 1.1$ Å^{-1} with a Be filter cooled to 77 K, collimations 30′/30′.

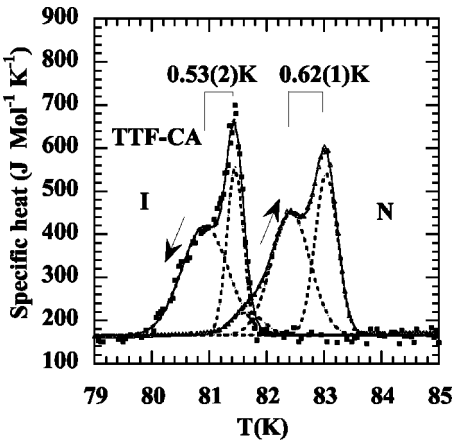

FIG. 5. C_p anomaly at the *N-I* transition of TTF-CA single crystals. △: observed as temperature increased at a constant heating rate $dT/dt = 0.2$ K/min ■: deduced during the natural cooling where dT/dt was about -0.27 K/min around $T_{N\text{-}I}$. The C_p anomaly is reproduced by a sum of Gaussian curves (dotted lines, Tables I and II) above a constant background, estimated as 166 J mol^{-1} K^{-1}.

such as either thermal cycling defects or not totally relaxed sticking strain, which may favor one of the phases with respect to the other.

Specific heat measurements were performed on TTF-CA single crystals. A hysteresis of about 1.5–2 K was observed for the specific heat (C_p) anomaly at the *N-I* transition. This multipeak C_p anomaly can be fitted by a sum of Gaussian curves (Fig. 5) from which enthalpy and entropy changes at the transition are deduced (Tables I and II). Three distinct peaks—two sharp and well-defined ones plus a third one which is rather a shoulder—have unambiguously been extracted from the curve measured with increasing temperature. In the curve obtained for decreasing temperature, the third peak is not visible. The two main C_p peaks are in good agreement with the double step behavior observed by neutron scattering: the difference of 0.57(2) K between the two largest peaks coincides with the length of the plateau observed on the evolution of the (030) reflection or on the integrated intensity of (020) Bragg peaks (Figs. 2 and 4). Moreover, each of the two main peaks of the C_p anomaly gives a fractional enthalpy change estimated between around 40 and 60 % of the total one (Table I and II). By using different heating rates it has been verified that this multipeak structure is intrinsic to the *N-I* instability and not caused by any temperature gradient which could cause parts of the sample to cross the transition one after another. These results are different from those published by Kawamura *et al.*,[43] where a single peak anomaly was observed in the adiabatic calorimetric response. In Fig. 2 of Ref. 43 the temperature steps used might have masked the multistep response. The anomaly we observe on single crystalline samples is significantly larger and less spread in temperature than the one observed with powder: highest peaks reach about 480 (Fig. 5) versus about 180 J mol.$^{-1}$ K^{-1} (Fig. 2 in Ref. 39), and temperature ranges where the multiple anomaly is observed are about 2.5 against 10 K. Consequently, the separation of

TABLE I. Multipeak C_p anomaly modeled by a sum of Gaussian curves. The parameters of the Gaussian curves are temperature, peak maximum and width. Enthalpy variation is deduced from the direct integration of each Gaussian curve. The estimate of entropy variation results from the integration of the function $C_P(T)/T=f(T)$.

Temperature increase	Shoulder	1st peak	2nd peak	Sum
Temperature (K)	81.65 ± 0.05	82.422 ± 0.007	83.039 ± 0.003	
Peak maximum ($J\,mol^{-1}\,K^{-1}$)	53 ± 7	284 ± 2	375 ± 9	
Width of the peak (K)	0.39 ± 0.04	0.48 ± 0.03	0.276 ± 0.004	
Entropy variation, ΔS ($J\,mol^{-1}\,K^{-1}$)	0.43 ± 0.03	2.90 ± 0.04	2.16 ± 0.02	5.49 ± 0.09
Enthalpy variation, ΔH ($J\,mol^{-1}$)	37 ± 9	240 ± 15	184 ± 7	461 ± 32
% of the total ΔH	8	52	40	100

the two principal peaks in C_p is here about 0.5 K, whereas 1.8 K were found for powdered samples. Such a dependence of the range of the transition temperature on the nature of the sample had already been observed by optical and spectroscopic measurements[28–30,44] and by nuclear quadrupolar resonance NQR.[33] Thus, it is known that the *N-I* instability is sensitive to both the crystal growth[29,30] and the crystalline state[33] (powder/single crystal). In the present case, the powder[39] was obtained from solution, the single crystals from cosublimation, and these two reasons explain the narrower temperature interval of the thermodynamical anomaly for single crystals. Nevertheless, the integrated intensities of the whole C_p anomaly in powder samples as well as in single crystals, no matter whether single peak[43] or multipeak structure (Ref. 39 and Tables I and II of the present work), are very similar, leading to the same strong entropy variation at the *N-I* transition, $8-9\times10^{-24}\ J\,K^{-1}$ per TTF-CA pair. This value is in good agreement with the entropy jump at the transition, which was evaluated from the Clapeyron equation using the (*P, T*) equilibrium line at atmospheric pressure.[25] Although close to $k_B \ln 2$, it should not be attributed to any order-disorder mechanism on a molecular scale, since no signature of such a phenomenon was indicated by diffraction, neither with x rays,[27] nor with neutrons.[20] This large entropy variation at $T_{N\text{-}I}$ may originate, on the one hand, from thermally induced lattice-relaxed CT excitations[24] and, on the other hand, from a change of vibrational entropy related to the volume variation at $T_{N\text{-}I}$ that is especially important along the **b** direction. We believe that for the sharply defined first-order temperature-induced transition at atmospheric pressure, (relatively low $T_{N\text{-}I}$), this second contribution should be the most significant one; this would be in consistency with the observed quasisystematic hardening of low-frequency acoustic and optical phonon modes in the *I* phase,[45,46] with respect to the *N* phase, due to closer interstack contacts (volume contraction).[20]

TABLE II. Multipeak C_p anomaly modeled by a sum of Gaussian curves. The parameters of the Gaussian curves are temperature, peak maximum and width. Enthalpy variation is deduced from the direct integration of each Gaussian curve. The estimate of entropy variation results from the integration of the function $C_P(T)/T=f(T)$.

Temperature decrease	1st peak	2nd peak	Sum
Temperature (K)	80.92 ± 0.02	81.448 ± 0.003	
Peak maximum ($J\,mol^{-1}\,K^{-1}$)	253 ± 6	391 ± 16	
Width of the peak (K)	0.57 ± 0.02	0.204 ± 0.008	
Entropy variation, ΔS ($J\,mol^{-1}\,K^{-1}$)	3.4 ± 0.1	1.72 ± 0.07	5.1 ± 0.2
Enthalpy variation, ΔH ($J\,mol^{-1}$)	257 ± 17	142 ± 11	398 ± 28
% of the total ΔH	64	36	100

In that context, and in order to investigate coexistence phenomena at a more macroscopic level, we have studied by optical microscopy the temperature-induced *N-I* transition, both in TTF-CA and in the less explored material TMB-TCNQ. In both materials, the phase transition shows up by a spectacular color change of the transmitted part of white light—yellow (*N* phase) to orange (*I* phase) for TTF-CA [Fig. 6(a)], light orange (*N* phase) to dark brown (*I* phase) for TMB-TCNQ [Fig. 6(b)]—in direct relation with the redshift of the optical absorption spectra.[14] Because of the well-marked first-order character of the temperature-induced transitions and, in addition, because of a temperature gradient on the samples resulting from the absorbed light, the coexistence of the *N* and the *I* phases extends over several degrees; no change of the orientation of the optical principal axes is observed. Moreover, this coexistence is associated with very clear geometric features at the *N-I* phase front. In both TTF-CA and TMB-TCNQ, the front is sharp and progresses across the crystal by jumps, but its orientation is different in the two materials. In TTF-CA, the phase front always appears as a macroscopic one, oriented perpendicularly to the **b** axis [Fig. 6(a)], which is a manner to reduce as much as possible long range elastic stress generated by the sharp **b** cell-parameter change at the transition (in agreement with the neutron scattering results presented in this paper). These phase fronts may also serve as seeds for domain walls between *I* domains of opposite polarization, giving rise to a

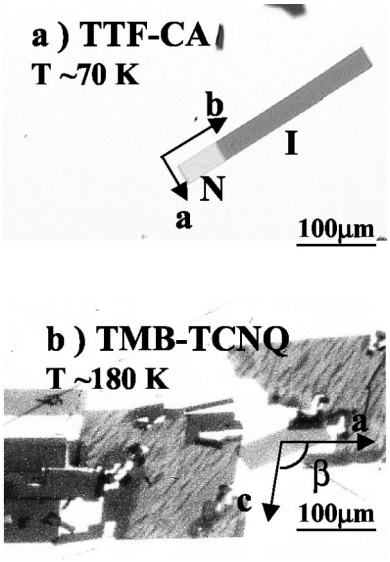

FIG. 6. The *N* and *I* phases observed by optical microscopy with unpolarized light. (a) Phase coexistence in TTF-CA around the *N-I* transition. (b) Transition-induced breaking of TMB-TCNQ crystals.

favorable energetic configuration, by decreasing electrostatic interactions between *I* domains. In TMB-TCNQ [Fig. 6(b)], narrow diagonal *I* domains appear in (**a**, **c**) planes whose number increases when temperature decreases. Such a coexistence is observed over several ten degrees Kelvin. However, when large parts of the crystal are fully transformed, the transition is always accompanied by a sharp breaking of the crystal along the **a** and **c** axes. Thus, it appears that elastic stress at the *N-I* transition is larger in TMB-TCNQ than in TTF-CA, with probably more important changes of the cell parameters, and that the TMB-TCNQ crystal does not succeed in relaxing this stress, at least not at atmospheric pressure. This feature, in addition to the difficulty to grow good crystals, explains why so few investigations have been carried out on this system. However, crystallographic structural studies would be essential for the understanding of the macroscopic transition mechanism in TMB-TCNQ.

CONCLUSION

Detailed structural investigations on TTF-CA around the temperature-induced *N-I* phase transition have provided essential insight and revealed a relevant scale, the mesoscopic one, to describe this uncommon electronic-structural multistability. There is no structural Devil's staircase associated with intermediate long periodicity structures with alternating *N* and *I* planes, in agreement with a recent *ab initio* calculation of the electrostatic energies. The coexistence at a mesoscopic scale, i.e., over more than 1000 Å, of both *N* and *I* phases is observed over slightly more than 2 K. A reproducible staging effect over about 0.5 K is observed thanks to the high experimental temperature stability, and it is very satisfying to notice the perfect coincidence between this step length and the gap separating the two main peaks observed for the specific heat anomaly. The coexistence of both the *N* and the *I* phase over about 2 K is caused by large elastic strain between the chains, mainly along the **b** direction, due to a strong coupling between electronic and structural changes. The two-step transition might be related to the well-marked first-order character of the temperature-induced transition which makes it difficult for the crystal to relax these elastic strains. The stored energy is released during a macroscopic *N-I* phase front jump. In TMB-TCNQ, elastic strains are also very crucial and at atmospheric pressure these are not relaxed but lead to a break of the sample. Under pressure, a two-step transition is observed by reflectivity measurements.[40] Details of the macroscopic mechanism could be clarified by precise structural studies only. A mesoscopic phase coexistence favored by interstack elastic coupling might occur as in TTF-CA. However, a recent *ab initio* calculation[42] of the electrostatic energies leads to the conclusion that in TMB-TCNQ, the staging state is slightly more stable than uniform *N* or *I* states.

[1] K. Nasu, in *Relaxations of Excited States and Photo-Induced Structural Phase Transitions*, edited by K. Nasu, Vol. 124 of *Springer-Series in Solid State Sciences* (Springer, Berlin, 1997).
[2] Y. Ogawa, S. Koshihara, K. Koshino, T. Ogawa, C. Urano, and H. Takagi, Phys. Rev. Lett. **84**, 3181 (2000).
[3] T. Tayagaki and K. Tanaka, Phys. Rev. Lett. **86**, 2886 (2001).
[4] S. Koshihara, Y. Tokura, Y. Iwasa, and T. Koda, Phys. Rev. B **44**, 431 (1991).
[5] S. Koshihara, Y. Tokura, T. Mitani, G. Saito, and T. Koda, Phys. Rev. B **42**, 6853 (1990).
[6] S. Koshihara, Y. Takahashi, H. Sakai, Y. Tokura, and T. Luty, J. Phys. Chem. B **103**, 2592 (1999).
[7] K. Tanimura and I. Akimoto, J. Lumin. **94–95**, 483 (2001).
[8] S. Iwai, S. Tanaka, K. Fujinuma, H. Kishida, H. Okamoto, and Y. Tokura, Phys. Rev. Lett. **88**, 057402 (2002).
[9] E. Collet, M. H. Lemée-Cailleau, M. Buron-Le Cointe, H. Cailleau, M. Wulff, T. Luty, S. Koshihara, M. Meyer, L. Toupet, P. Rabiller, and S. Techert, Science **300**, 612 (2003).
[10] Y. Iwasa, T. Koda, Y. Tokura, S. Koshihara, N. Iwasawa, and G. Saito, Appl. Phys. Lett. **55**, 2111 (1989).
[11] Y. Tokura, H. Okamoto, T. Koda, T. Mitani, and G. Saito, Phys. Rev. B **38**, 2215 (1988).
[12] N. Watanabe, Y. Iwasa, and T. Koda, Phys. Rev. B **44**, 11 111 (1991).
[13] R. Kumai, Y. Okimoto, and Y. Tokura, Science **284**, 1645 (1999).
[14] J. B. Torrance, J. E. Vasquez, J. J. Mayerle, and V. Y. Lee, Phys. Rev. Lett. **46**, 253 (1981).
[15] Y. Iwasa, T. Koda, Y. Tokura, A. Kobayashi, N. Iwasana, and G. Saito, Phys. Rev. B **42**, 2374 (1990).
[16] S. Aoki, T. Nakayama, and A. Miura, Phys. Rev. B **48**, 626 (1993).
[17] S. Aoki and T. Nakayama, Phys. Rev. B **56**, 2893 (1997).
[18] T. Hasegawa, T. Akutagawa, T. Nakamura, T. Mochida, R. Kondo, S. Kagoshima, and Y. Iwasa, Phys. Rev. B **64**, 085106

(2001).
[19] L. Farina, A. Brillante, M. Masino, and A. Girlando, Phys. Rev. B **64**, 144102 (2001).
[20] M. Le Cointe, M. H. Lemée-Cailleau, H. Cailleau, B. Toudic, L. Toupet, G. Heger, F. Moussa, P. Schweiss, K. H. Kraft, and N. Karl, Phys. Rev. B **51**, 3374 (1995).
[21] N. Nagaosa, J. Phys. Soc. Jpn. **55**, 3488 (1986).
[22] H. Cailleau, T. Luty, M. H. Lemée-Cailleau, E. Collet, M. Buron-Le Cointe, E. Zienkiewicz, and F. Moussa, in *Frontiers of High Pressure Research II: Application of High Pressure to Low-Dimensional Novel Electronic Materials*, edited by H. D. Hochheimer *et al.*, Nato Science Series (Kluwer, Dordrecht, 2001), pp. 167–178.
[23] T. Luty, H. Cailleau, S. Koshihara, E. Collet, M. Takesada, M. H. Lemée-Cailleau, M. Buron-Le Cointe, N. Nagaosa, Y. Tokura, E. Zienkiewicz, and B. Ouladdiaf, Europhys. Lett. **59**, 619 (2002).
[24] E. Collet, M. H. Lemée-Cailleau, M. Buron-Le Cointe, H. Cailleau, S. Ravy, T. Luty, J. F. Bérar, P. Czarnecki, and N. Karl, Europhys. Lett. **57**, 67 (2002).
[25] M. H. Lemée-Cailleau, M. Le Cointe, H. Cailleau, T. Luty, F. Moussa, J. Roos, D. Brinkmann, B. Toudic, C. Ayache, and N. Karl, Phys. Rev. Lett. **79**, 1690 (1997).
[26] H. Cailleau, E. Collet, T. Luty, M. H. Lemée-Cailleau, M. Buron-Le Cointe, and S. Koshihara, in *Multiphoton and Light Driven Multielectron Processes in Organics: New Phenomena, Materials and Applications*, edited by F. Kajzar and M. V. Agranovich (Kluwer Academic, Dordrecht, 2000), p. 451.
[27] J. J. Mayerle, J. B. Torrance, and J. I. Crowley, Acta Crystallogr., Sect. B: Struct. Crystallogr. Cryst. Chem. **35**, 2988 (1979).
[28] C. S. Jacobsen and J. B. Torrance, J. Chem. Phys. **78**, 112 (1983).
[29] K. Kikuchi, K. Yakushi, and H. Kuroda, Solid State Commun. **44**, 151 (1982).
[30] Y. Tokura, T. Koda, T. Mitani, and G. Saito, Solid State Commun. **43**, 757 (1982).
[31] H. Bartholin, J. L. Baudour, C. Breandon, R. Tchapoutian, H. Cailleau, and D. Perrin, Solid State Commun. **63**, 223 (1987).
[32] M. H. Lemée-Cailleau, B. Toudic, H. Cailleau, F. Moussa, M. Le Cointe, G. Silly, and N. Karl, Ferroelectrics **127**, 19 (1992).
[33] J. Gallier, B. Toudic, Y. Délugeard, H. Cailleau, M. Gourdji, A. Péneau, and L. Guibé, Phys. Rev. B **47**, 11 688 (1993); M. Le Cointe, J. Gallier, H. Cailleau, M. Gourdji, A. Péneau, and L. Guibé, Solid State Commun. **94**, 455 (1995).
[34] Y. Yoshinari, Y. Maniwa, T. Takahashi, K. Mizoguchi, and T. Mitani, Synth. Met. **19**, 521 (1987).
[35] B. Toudic, J. Gallier, M. Boumaza, and H. Cailleau, J. Phys. (France) **51**, 1671 (1990).
[36] A. Girlando, F. Marzola, C. Pecile, and J. B. Torrance, J. Chem. Phys. **79**, 1075 (1983).
[37] J. Hubbard and J. B. Torrance, Phys. Rev. Lett. **47**, 1750 (1981).
[38] R. Bruinsma, P. Bak, and J. B. Torrance, Phys. Rev. B **27**, 456 (1983).
[39] C. Ayache and J. B. Torrance, Solid State Commun. **47**, 789 (1983).
[40] Y. Iwasa, N. Watanabe, T. Koda, and G. Saito, Phys. Rev. B **47**, 2920 (1993).
[41] E. Collet, M. Buron-Le Cointe, M. H. Lemée-Cailleau, H. Cailleau, L. Toupet, M. Meven, S. Mattauch, G. Heger, and N. Karl, Phys. Rev. B **63**, 054105 (2001).
[42] T. Iizuka-Sakano, T. Kawamoto, Y. Shimoi, and S. Abe, Phase Transit. **75**, 831 (2002).
[43] T. Kawamura, Y. Miyazaki, and M. Sorai, Chem. Phys. Lett. **273**, 435 (1997).
[44] J. B. Torrance, A. Girlando, J. J. Mayerle, J. I. Crowley, V. Y. Lee, and P. Batail, Phys. Rev. Lett. **47**, 1747 (1981).
[45] A. Moréac, A. Girard, Y. Délugeard, and Y. Marqueton, J. Phys.: Condens. Matter **8**, 3553 (1996).
[46] E. Collet, Y. Marqueton, M. H. Lemée-Cailleau, and P. Roy (private communication).